On the mechanism of gold NHC compounds binding to DNA G-quadruplexes elucidated by combined metadynamics and biophysical methods

Darren Wragg,[+a] Andreia de Almeida,[+a] Riccardo Bonsignore,[+a] Fritz E. Kühn,[b] Stefano Leoni*[a] and Angela Casini*[a,c]

Abstract: The binding modes and free-energy landscape of two Au(I) N-heterocyclic carbene complexes interacting with G-quadruplexes, namely a human telomeric (hTelo) and a promoter (*C-KIT1*) sequence, are studied here for the first time by metadynamics. The theoretical results are validated by FRET DNA melting assays and provide an accurate estimate of the absolute gold complex/DNA binding free energy. This advanced *in silico* approach is valuable to achieve rational drug design of selective G4s binders.

DNA can adopt different structures other than the canonical right-handed double helix (B-DNA), and numerous structural studies have revealed that guanine-rich DNA sequences can form secondary structures termed G-quadruplexes (G4s).[1] To form G4s, four guanine bases assemble into a pseudoplanar tetrad (G-quartet) are held together by one or more nucleotide strands and stabilized by metal ions. Recent bioinformatics studies have shown that there are ca. 716,000 DNA sequences in the human genome that can potentially form G4 structures.[2] These non-canonical DNA structures are present in telomeres and promoter regions of oncogenes and have been the subject of intense study over the past 10 years, being associated with a number of biological processes such as telomere maintenance, gene regulation, and replication.[3] It has been proposed that formation of the quadruplex structure in promoter regions can control transcription and, as a consequence, the expression of the corresponding oncogenes.[4] Moreover, stabilizing G4s in telomeres indirectly inhibits telomerase activity, thus affecting cancer mortality.[3b]

Within this context, G4s emerge as promising targets for anticancer drug discovery, while their roles in cancer biology have yet to be completely elucidated. A number of studies report on the efficient G4 stabilization by small molecules with associated anticancer effects.[5] For example, the tri-substituted acridine derivative, BRACO-19, a telomeric G4 stabilizer, has shown *in vitro* anticancer activity in prostate cancer. [6] Of note, two quinolone molecules, CX-3543 and CX-5461, selectively stabilize G4s structures, and are now in clinical trials.[7]

In addition to organic molecules, metal-based compounds have also been developed as promising experimental G4 stabilizers, including several Schiff-base metal complexes (mainly Ni^{2+},[8] Cu^{2+},[8c-e] Zn^{2+},[8a-c] Pt^{2+} [9] and Pt^{4+} [9a]), as well as some metallo-supramolecular DNA-binders.[10] Despite the great advances in the development of G4 stabilizers, still important challenges remain to be tackled, including achieving selective binding of small molecules to a specific quadruplex over duplex DNA and other G4s.

Our pioneering work in this area identified small-molecule organometallic Au(I) compounds, featuring N-heterocyclic carbenes (NHCs) ligands, as potent and selective stabilizers of telomeric G4s,[11] including the bis-NHC gold(I) complex - $[Au(9\text{-methylcaffein-8-ylidene})_2]^+$ (**$AuTMX_2$**, Figure 1).[11a] X-ray diffraction analysis of the adduct formed by **$AuTMX_2$** and a 23-nucleotide telomere repeat sequence (Tel23) indicated that the compound binds non-covalently between neighbouring G4s.[11b]

Based on these promising results, our research in an unmet medical need involves developing new organometallic Au(I) NHC complexes targeting specific G4 structures for possible applications in therapy and/or imaging. In order to rationally achieve selectivity, computational methods, including molecular dynamics (MD) approaches, are highly valuable in elucidating both the structural and energetics requisites underlying the ligand/target recognition process. In fact, a number of classical MD studies on the adducts of G4s structures with different stabilizers have been performed providing atomistic support for the interpretation of the binding mechanism to G4-DNA.[8a-c, 12]

Recently, funnel-metadynamics has been shown to be successful at calculating the free energy surface for organic ligands and their interactions with G4s.[13] Thus, we applied

[a] D. Wragg,[+] Dr. A. de Almeida,[+] Dr. R. Bonsignore,[+] Dr. S. Leoni, Prof. A. Casini
School of Chemistry
Cardiff University
Park Place, CF10 3AT Cardiff, United Kingdom
E-mail: LeoniS@cardiff.ac.uk and CasiniA@cardiff.ac.uk
[b] Prof. F. Kühn
Molecular Catalysis, Department of Chemistry, Catalysis Research Center
Technische Universität München
Lichtenbergstr. 4, 85747 Garching bei München, Germany
[c] Prof. A. Casini
Institute for Advanced Study
Technische Universität München
Lichtenbergstr. 2a, 85747 Garching bei München, Germany
[+] These authors contributed equally to the work

Supporting information for this article is given via a link at the end of the document.

metadynamics to evaluate the binding of **AuTMX$_2$** to two different G4 structures, namely the human telomeric sequence hTelo (pdb 2HY9[14]) and the *C-KIT1* oncogene promoter sequence (pdb 4WO2[15]). The results have been compared with those obtained for the neutral mono-carbene complex **AuTMX-I** (Figure 1). Furthermore, we have validated the accuracy of our calculations performing gold complexes/G4 binding assays using FRET (fluorescence resonance energy transfer) DNA melting.

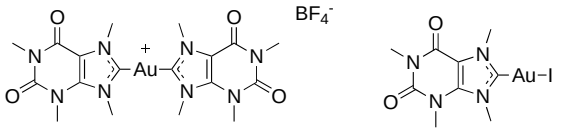

AuTMX$_2$ **AuTMX-I**

Figure 1. Chemical structures of the two Au(I) NHCs investigated in this study.

Initially, the X-ray structure of the telomeric-G4 adduct with **AuTMX$_2$** (pdb 5CCW[11b]) was used as reference to run a first set of metadynamics simulations, to calculate the compound's thermodynamically most stable positions, providing a starting point for the free energy calculations with hTelo and *C-KIT1* (see Experimental for details). This allowed the validation and positioning of the interaction of **AuTMX$_2$** with the selected G4 models (Figure S1). In our study, the Gibbs-free energy (at 300 K, ΔG_{MD}) was determined for all the seven compound's poses (Table S1) and showed that each one has different binding energy. The position corresponding to the **AuTMX$_2$**'s interaction with the topmost tetrad (pose 1, Figure S1), was chosen for the further calculations of the interactions with hTelo and *C-KIT1.*

In the work of Moraca et al., funnel metadynamics was used to constrain the ligand within a specific area determined to be the top tetrad surface.[13] However, in our study, the gold-complexes were not constrained and were allowed to find the most energetically favourable interactions with the entire G4 models, including loops and top and bottom tetrads, allowing possible further interactions to be identified. Thus, five 50 ns trajectories were calculated for each combination of compound and G4 model (for a total of 4 experimental conditions and a total of 20 simulations). This was performed using a simple distance collective variable (CV) between the Au^+ centre of the complex and the K^+ at the centre of the uppermost tetrad (see experimental section for details), resulting in a free-energy (ΔG_{MD}, at 300 K) profile output, based on the Au^+-K^+ distance (Figure S2, Table 1). Moreover, to closely investigate the molecular mechanism of interaction of the gold complexes, multi-CV calculations were run on the same systems. This involved adding a second CV for the torsion angle between the complexes and the uppermost tetrads (Figure 2).

As metadynamics explores the whole energy surface of an interaction, rather than just one minimum, further possible meta-stable positions can also be observed. In fact, hTelo's trajectories with **AuTMX$_2$** show two possible binding sites (state **I** and **II**) with the first one (state **I**) having the lowest energy (ca. -37 KJ/mol, Table 1). Figures 2 shows the multiple collective variable (CV) plot of free energy surface of **AuTMX$_2$** interactions with hTelo. Interestingly, state **I** shows two minima (**a** and **b**), corresponding to the same Au-K^+ distance (ca. 0.8 nm) but with different torsion angles. The latter are related to **AuTMX$_2$** being virtually in the same position but with the gold complex rotating around its centre, resulting in the same pose with two different torsion angles (see position of the caffeine ligands in Figure 2).

In state **I**, **AuTMX$_2$** is interacting with both an adenine (A13) in the loop b region, and two guanine bases of the tetrad (G4 and G22), with strong π-stacking between the NHCs of the gold complex and the aromatic rings of G22 (Figure 2). Instead, the higher energy state **II** (ca. -14 KJ/mol, Table 1) corresponds to a position where the gold complex does not interact with the guanine bases, but exclusively with the loop thymine (T11) (Figure 2). In this second state, the loop covers the top of the G4-tetrad, hindering possible interactions between the gold complex and the G-tetrad.

Interestingly, a similar behaviour was observed for **AuTMX$_2$** binding to *C-KIT1*, with two states **I** and **II** (Figure S3, Table 1). *C-KIT1* has a very different structure and surface from hTelo: while the former has a prominent flanking loop that may cover the top of the tetrad, *C-KIT1* top surface is virtually flat, leading the gold complex to interact with the top of the tetrad and the rings of flanking bases (A1) (Figure S3). Thus, state **I** corresponds to **AuTMX$_2$** stabilized by π-stacking with the guanine rings (lowest energy), while in state **II**, it interacts with both A1 and G6 via π-stacking (Figure S3).

When the simulation was repeated for the neutral mono-NHC complex **AuTMX-I**, the compound was shown to interact via π-π and π-alkyl interactions with the guanine tetrad (G22) and the loop (A13) in hTelo (Figure S4), as observed for **AuTMX$_2$** (state **I**). However, as expected, the calculated ΔG_{MD} was lower with respect to the one for **AuTMX$_2$**, due to the lack of the second caffeine ligand (Table 1). The enhanced efficiency of multiple collective variable simulations proved extremely valuable in identifying a second, unexpected binding mode of **AuTMX-I** (state **II**), similar in energy to state **I**. Therein, the complex interacts within a grove in loop c (Figure S4) by π-π stacking the caffeine moiety with T18. This interaction was only observed when using the multiple collective variable simulations.

With *C-KIT1,* **AuTMX-I** shows a single binding mode due to its π-stacking with G6 of the uppermost tetrad of the G4 (Figure S5). Moreover, the iodido ligand tends to be positioned outside the G4 structure, in both hTelo and *C-KIT1* adducts.

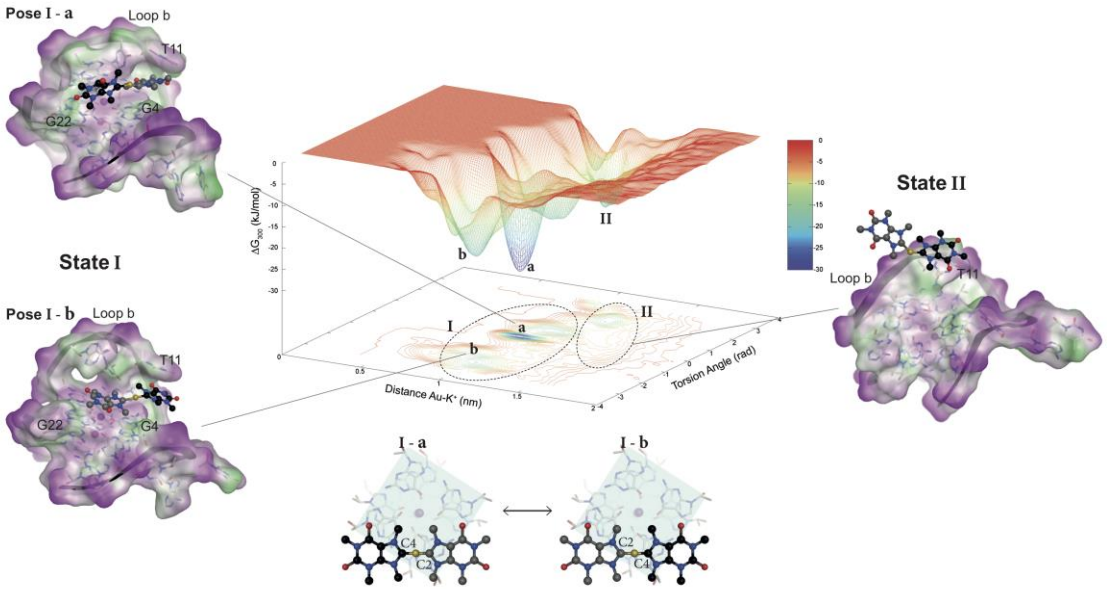

Figure 2. Multiple collective variable (CV) plot of free energy surface of **AuTMX₂** interactions with hTelo (centre). CVs correspond to distance (nm) between Au^+ in **AuTMX₂** and K^+ in upper tetrad and torsion angle (rad). Two states are highlighted (**I** and **II**) and two poses for state **I** are shown as **a** and **b**. States **I-a, b** and **II** are shown in translucent molecular surface, coloured according to lipophilicity (green: lipophilic, pink: hydrophilic). G4 structure is shown as sticks and ribbon, with hidden backbone for clarity. **AuTMX₂** is shown in ball and stick, with each caffeine ligand coloured differently (black and grey). C2 and C4 highlight the carbon atom positions in **AuTMX₂** in each of the related poses **I-a** or **I-b**.

Table 1. Gibbs-free energy values, experimental (ΔG_{exp}) and calculated by metadynamics (ΔG_{MD}), for **AuTMX₂** and **AuTMX-I** interactions with hTelo and *C-KIT1*. ΔG values are expressed in kJ/mol and obtained considering T = 300K. Experimental binding constants (K_b) are reported in Table S2.

	G4 model			
	hTelo		*C-KIT1*	
	ΔG_{MD}[a]	ΔG_{exp}	ΔG_{MD}[a]	ΔG_{exp}
AuTMX₂ (state I)	-37 ± 7	-39 ± 2	-45 ± 3	-37.6 ± 0.4
AuTMX₂ (state II)	-14 ± 3	-12.1 ± 0.4	-12 ± 3	-
AuTMX-I	-28 ± 3	-23.2 ± 0.4	-30 ± 5	-29 ± 3

[a] Data are obtained from simulations using a simple distance collective variable.

Following the interesting observations of multiple binding modes of **AuTMX₂** and to further investigate the stabilization properties of the two gold-based complexes, determination of the Gibbs-free energy (ΔG_{exp}) from the DNA FRET melting profiles was performed. Thus, **AuTMX₂** and **AuTMX-I** were synthesized by adapting published protocols. [11a, 16] starting from their methylated precursors (Scheme S1 and S2). The difference in DNA melting temperature (ΔT_m, in °C) of hTelo and *C-KIT1* induced by the binding of the two Au(I) NHC complexes was readily monitored through the modification of the FRET phenomenon and enabled an easy quantification of the compounds' stabilization properties of G4-DNA. Afterwards, the compounds were incubated with fixed amounts of each G4 for 10 min and the DNA melting profile recorded. As shown in Figure 3, both complexes stabilize the hTelo and *C-KIT1* structures, with the strongest effects observed for **AuTMX₂**.

As previously reported,[11c] **AuTMX₂** leads to a characteristic melting profile for hTelo, featuring a two-step melting pattern, where a small increase in fluorescence is initially observed before the steep increase after ca. 65 ºC (Figure 3A, red trace). Instead, **AuTMX₂** with *C-KIT1,* investigated for the first time, shows a gradually incrementing curve, rather than an initial steep ramp or two-step curve.

In the presence of the mono-caffeine derivative, **AuTMX-I**, the ΔT_m of both G4s is approximately 2-fold lower than the one found for **AuTMX₂** (6.5 ± 0.2 ºC for hTelo and 11.0 ± 1.8 ºC for *C-KIT1*, respectively). Interestingly, **AuTMX-I** does not have an effect on the shape of the melting profiles of either DNA sequence, which is similar to the control DNA (Figure 3A-B, black and blue traces).

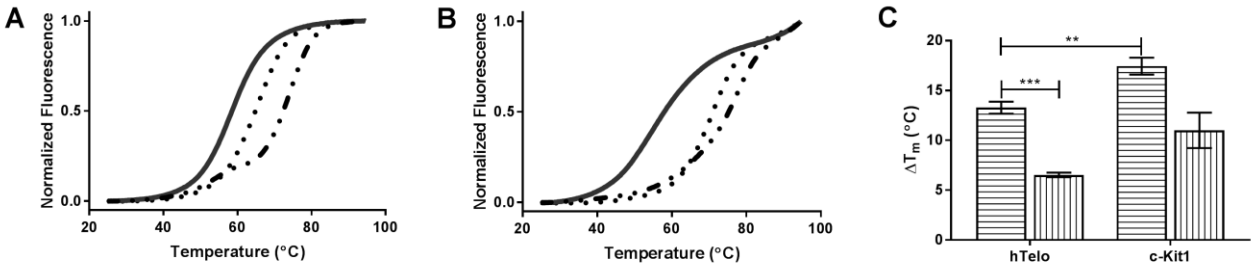

Figure 3. Representative FRET melting profiles of a 0.2 μM hTelo (A) and C-KIT1 (B) G-quadruplex DNA solutions in 60 mM potassium cacodylate buffer in absence (black solid lines), and in presence of 1 μM of **AuTMX$_2$** (dotted lines) and **AuTMX-I** (dashed lines). C) ΔT_m of hTelo and C-KIT1 G4s in the presence of **AuTMX$_2$** (horizontal lines) and **AuTMX-I** (vertical lines). Data is shown as mean ± SEM of three independent experiments; ** p<0.005, *** p<0.001. Results for **AuTMX-I** hTelo *vs* C-KIT1 are significantly different (significance not shown in the plot), * p<0.05.

In order to determine the energy of binding (ΔG_{exp}) of the gold compounds to each G4, the experimental data were normalized to folded fraction (θ) of G4-DNA and fitted according to Eq. 1 and 2,[17] where the enthalpy (ΔH) for the process was derived from the resulting fit (see Experimental section). In order to fit a two-step melting profile of **AuTMX$_2$** with hTelo, another equation (Eq. 4, Experimental section) was used, taking into account the upper and lower limits of the sigmoid curve used for fitting. This allowed us to treat the data fits as two independent melting curves. Thus, ΔG_{exp} was calculated for both compounds vs each G4 structure, and also for hTelo's two-step melting curve (Table 1). The resulting fits are shown in Figure S6. From the reported results a trend could also be identified in which the greater the stabilization of the G4 structure by the compound and lower is the energy of binding (at least considering the most stable mode, state **I** for hTelo).

Most importantly, the ΔG_{exp} are in perfect accordance with the ΔG_{MD} values obtained using metadynamics (Table 1). The analysis of the melting curves and ΔG_{exp} values of **AuTMX$_2$** with the two G4 models clearly suggest the existence of two distinct modes of binding, possibly mutually exclusive, in line with the computational results. Thus, considering hTelo, the first binding mode corresponds to the lower energy state **I** (Figures 2 and S6), exclusively featuring compound's interaction with the guanines in the tetrad. The second binding mode at higher energy (state **II**) involves loop/flanking base interactions and/or interactions with part of the tetrad (Figures 2 and S6). Instead, as observed before, the flatness of the top tetrad of *C-KIT1* allows the compound to probe the whole top-surface of the G4. Since the stacking of the complex with the guanines is more favourable (state **I**), it may be expected that this is the interaction most likely to occur *in vitro*. Notably, our metadynamics results also point towards the existence of a second binding site for **AuTMX-I** on hTelo, involving the loop C. This interaction may be for further optimization of selective hTelo stabilizers.

Overall, the *in silico* results confirm and complement the experimental data revealing two ligand binding modes of **AuTMX$_2$** on the two G4s structures, and providing further structural and energetics information on ligand binding mechanism, including a quantitatively well-characterized free-energy landscape. The experimental validation of the binding energy of Au(I) NHC to G4s complexes calculated by metadynamics methods was also achieved. This advanced approach can be extended to other types of molecules as G4 stabilizers, highlighting selectivity features essential to orient the drug design.

Acknowledgements

A.C. acknowledges support from Cardiff University and the Hans Fischer Senior Fellowship of the Technical University of Munich – Institute for Advanced Study, funded by the German Excellence Initiative and the European Union Seventh Framework Program, under grant agreement n° 291763. R.B. acknowledges funding from the European Union's Horizon 2020 research and innovation program under the Marie Skłodowska-Curie grant agreement nº 663830. This work has been performed using resources provided by the "Cambridge Service for Data Driven Discovery" (CSD3, http://csd3.cam.ac.uk) system operated by the University of Cambridge Research Computing Service (http://www.hpc.cam.ac.uk) funded by EPSRC Tier-2 capital grant EP/P020259/1. We gratefully acknowledge the support of NVIDIA Corporation with the donation of a Quadro P5000 GPU used for this research.

Keywords: gold N-heterocyclic carbenes • G-quadruplexes • metadynamics • FRET DNA melting • cancer

References

[1] D. Monchaud, M. P. Teulade-Fichou, *Org Biomol Chem* **2008**, *6*, 627-636.

[2] V. S. Chambers, G. Marsico, J. M. Boutell, M. Di Antonio, G. P. Smith, S. Balasubramanian, *Nature biotechnology* **2015**, *33*, 877-881.

[3] aD. Rhodes, H. J. Lipps, *Nucleic acids research* **2015**, *43*, 8627-8637; bA. Bernal, L. Tusell, *International journal of molecular sciences* **2018**, *19*, 294.

[4] S. Neidle, in *Therapeutic Applications of Quadruplex Nucleic Acids*, Academic Press, Boston, **2012**, pp. 119-138.

[5] S. Balasubramanian, L. H. Hurley, S. Neidle, *Nature reviews. Drug discovery* **2011**, *10*, 261-275.

[6] C. M. Incles, C. M. Schultes, H. Kempski, H. Koehler, L. R. Kelland, S. Neidle, *Molecular cancer therapeutics* **2004**, *3*, 1201-1206.

[7] H. Xu, M. Di Antonio, S. McKinney, V. Mathew, B. Ho, N. J. O'Neil, N. D. Santos, J. Silvester, V. Wei, J. Garcia, F. Kabeer, D. Lai, P. Soriano, J. Banath, D. S. Chiu, D. Yap, D. D. Le, F. B. Ye, A. Zhang, K. Thu, J. Soong, S. C. Lin, A. H. Tsai, T. Osako, T. Algara, D. N. Saunders, J. Wong, J. Xian, M. B. Bally, J. D. Brenton, G. W. Brown, S. P. Shah, D. Cescon, T. W. Mak, C. Caldas, P. C. Stirling, P. Hieter, S. Balasubramanian, S. Aparicio, *Nature communications* **2017**, *8*, 14432.

[8] aR. Bonsignore, F. Russo, A. Terenzi, A. Spinello, A. Lauria, G. Gennaro, A. M. Almerico, B. K. Keppler, G. Barone, *Journal of inorganic biochemistry* **2018**, *178*, 106-114; bR. Bonsignore, A. Terenzi, A. Spinello, A. Martorana, A. Lauria, A. M. Almerico, B. K. Keppler, G. Barone, *Journal of inorganic biochemistry* **2016**, *161*, 115-121; cA. Terenzi, R. Bonsignore, A. Spinello, C. Gentile, A. Martorana, C. Ducani, B. Hogberg, A. M. Almerico, A. Lauria, G. Barone, *RSC Advances* **2014**, *4*, 33245-33256; dA. Terenzi, D. Lotsch, S. van Schoonhoven, A. Roller, C. R. Kowol, W. Berger, B. K. Keppler, G. Barone, *Dalton transactions* **2016**, *45*, 7758-7767; eN. H. Campbell, N. H. Karim, G. N. Parkinson, M. Gunaratnam, V. Petrucci, A. K. Todd, R. Vilar, S. Neidle, *J.Med.Chem.* **2012**, *55*, 209-222; fC. Q. Zhou, T. C. Liao, Z. Q. Li, J. Gonzalez-Garcia, M. Reynolds, M. Zou, R. Vilar, *Chemistry* **2017**, *23*, 4713-4722.

[9] aS. Bandeira, J. Gonzalez-Garcia, E. Pensa, T. Albrecht, R. Vilar, *Angewandte Chemie Int. Ed.* **2018**, *57*, 310-313; bA. D. L., H. B. W. J., C. Leticia, M. Oscar, V. Ramon, A. W. Janice, *Chemistry –Eur. J.* **2016**, *22*, 2317-2325.

[10] aP. Wu, D. L. Ma, C. H. Leung, S. C. Yan, N. Zhu, R. Abagyan, C. M. Che, *Chemistry* **2009**, *15*, 13008-13021; bS. Ghosh, O. Mendoza, L. Cubo, F. Rosu, V. Gabelica, A. J. White, R. Vilar, *Chemistry* **2014**, *20*, 4772-4779; cX. H. Zheng, H. Y. Chen, M. L. Tong, L. N. Ji, Z. W. Mao, *Chemical communications* **2012**, *48*, 7607-7609; dX. H. Zheng, Y. F. Zhong, C. P. Tan, L. N. Ji, Z. W. Mao, *Dalton transactions* **2012**, *41*, 11807-11812.

[11] a B. Bertrand, L. Stefan, M. Pirrotta, D. Monchaud, E. Bodio, P. Richard, P. Le Gendre, E. Warmerdam, M. H. de Jager, G. M. Groothuis, M. Picquet, A. Casini, *Inorganic chemistry* **2014**, *53*, 2296-2303; b C. Bazzicalupi, M. Ferraroni, F. Papi, L. Massai, B. Bertrand, L. Messori, P. Gratteri, A. Casini, *Angewandte Chemie* **2016**, *55*, 4256-4259; c L. Stefan, B. Bertrand, P. Richard, P. Le Gendre, F. Denat, M. Picquet, D. Monchaud, *Chembiochem* **2012**, *13*, 1905-1912.

[12] aE. D. M., S. L. M., C. G. H., *Chemistry –Eur. J.* **2018**, *24*, 2117-2125; bM. Kanti Si, A. Sen, B. Ganguly, *Physical Chemistry Chemical Physics* **2017**, *19*, 11474-11484.

[13] F. Moraca, J. Amato, F. Ortuso, A. Artese, B. Pagano, E. Novellino, S. Alcaro, M. Parrinello, V. Limongelli, *PNAS* **2017**, *114*, E2136-e2145.

[14] J. Dai, C. Punchihewa, A. Ambrus, D. Chen, R. A. Jones, D. Yang, *Nucleic acids research* **2007**, *35*, 2440-2450.

[15] D. Wei, J. Husby, S. Neidle, *Nucleic acids research* **2015**, *43*, 629-644.

[16] A. Kascatan-Nebioglu, A. Melaiye, K. Hindi, S. Durmus, M. J. Panzner, L. A. Hogue, R. J. Mallett, C. E. Hovis, M. Coughenour, S. D. Crosby, A. Milsted, D. L. Ely, C. A. Tessier, C. L. Cannon, W. J. Youngs, *JMedChem* **2006**, *49*, 6811-6818.

[17] A. Bottcher, D. Kowerko, R. K. Sigel, *Biophysical chemistry* **2015**, *202*, 32-39.

Entry for the Table of Contents

Layout 1:

COMMUNICATION

Gold organometallics as selective G-quadruplex stabilizers.

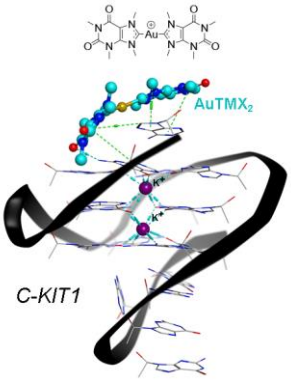

*Author(s), Corresponding Author(s)**

Page No. – Page No.

Title